Discovery of a Strongly Phase-variable Spectral Feature in the Isolated Neutron Star RX J0720.4-3125

Borghese, A.; Rea, N.; Coti Zelati, F.; Tiengo, A.; Turolla, R.

DOI
10.1088/2041-8205/807/1/L20

Publication date
2015

Document Version
Final published version

Published in
Astrophysical Journal Letters

The Astrophysical Journal Letters, 807:L20 (5pp), 2015 July 1 doi:10.1088/2041-8205/807/1/L20

DISCOVERY OF A STRONGLY PHASE-VARIABLE SPECTRAL FEATURE IN THE ISOLATED NEUTRON STAR RX J0720.4–3125

A. Borghese[1], N. Rea[1,2], F. Coti Zelati[1,3,4], A. Tiengo[5,6,7], and R. Turolla[8,9]
[1] Anton Pannekoek Institute for Astronomy, University of Amsterdam, Postbus 94249, NL-1090 GE Amsterdam, The Netherlands
[2] Institute of Space Sciences (CSIC-IEEC), Carrer de Can Magrans S/N, E-08193 Barcelona, Spain
[3] Università dell'Insubria, via Valleggio 11, I-22100 Como, Italy
[4] INAF-Osservatorio Astronomico di Brera, via Bianchi 46, I-23807 Merate (LC), Italy
[5] INAF-Istituto di Astrofisica Spaziale e Fisica Cosmica, via E. Bassini 15, I-20133 Milano, Italy
[6] Istituto Universitario di Studi Superiori, piazza della Vittoria 15, I-27100 Pavia, Italy
[7] Istituto Nazionale di Fisica Nucleare, Sezione di Pavia, via A. Bassi 6, I-27100 Pavia, Italy
[8] Dipartimento di Fisica e Astronomia, Università di Padova, via F. Marzolo 8, I-35131 Padova, Italy
[9] Mullard Space Science Laboratory, University College London, Holmbury St. Mary, Dorking, Surrey RH5 6NT, UK
Received 2015 April 23; accepted 2015 June 12; published 2015 July 1

ABSTRACT

We present the discovery of a strongly phase-variable absorption feature in the X-ray spectrum of the nearby, thermally emitting, isolated neutron star RX J0720.4–3125. The absorption line was detected performing detailed phase-resolved spectroscopy in 20 *XMM-Newton* observations, covering the period 2000 May–2012 September. The feature has an energy of ∼750 eV, an equivalent width of ∼30 eV, and it is significantly detected for only ∼20% of the pulsar rotation. The absorption feature appears to be stable over the timespan covered by the observations. Given its strong dependence on the pulsar rotational phase and its narrow width, a plausible interpretation is in terms of resonant proton cyclotron absorption/scattering in a confined magnetic structure very close to the neutron star surface. The inferred field in such a magnetic loop is $B_{\rm loop} \sim 2 \times 10^{14}$ G, a factor of ∼7 higher than the surface dipolar magnetic field.

Key words: stars: individual (RX J0720.4–3125) – stars: neutron – X-rays: stars

1. INTRODUCTION

RX J0720.4–3125 belongs to a group of seven thermally emitting, radio-quiet, and nearby ($\lesssim$500 pc) isolated neutron stars, originally discovered in *ROSAT* all-sky survey data, and often referred to as the X-ray dim isolated neutron stars (XDINSs). They are among the closest known neutron stars, and are characterized by X-ray luminosities $L_{\rm X} \approx 10^{30-33}$ erg s^{-1}, long spin periods ($P \sim$ 3–11 s), and inferred surface dipolar magnetic fields $B_{\rm dip} \approx 10^{13}$ G, partially overlapping those of the magnetars (see van Kerkwijk & Kaplan 2007 and Turolla 2009 for reviews). XDINSs have estimated ages of a few 10^5 years, derived from cooling curves and kinematics, while the characteristic ages are somewhat longer (∼10^6 years). The X-ray spectra show thermal emission with inferred temperatures $kT \approx$ 50–100 eV and lack the non-thermal, power-law component often observed in other isolated neutron stars. Although a blackbody model provides an overall good description of their X-ray spectra, broad absorption features have been found in six of the XDINSs with *XMM-Newton* observations. Their origin is unclear: they can be produced either by proton cyclotron resonances/atomic transitions in a magnetized atmosphere, or by an inhomogeneous surface temperature distribution, as recently suggested by Viganò et al. (2014).

RX J0720.4–3125, the second brightest member of the class, was discovered by Haberl et al. (1997) as an isolated, pulsating neutron star with an 8.39 s spin period. The X-ray spectrum is best modeled by a blackbody ($kT \sim$ 85 eV) plus a broad (∼70 eV wide) absorption feature centered at ∼270 eV (Haberl et al. 2004). A further, narrow (∼5 eV wide) line was identified in *XMM-Newton* Reflection Grating Spectrometer data at ∼570 eV (Hohle et al. 2012a and references therein), possibly due to Oxygen circumstellar/interstellar absorption. Unlike other XDINSs, RX J0720.4–3125 exhibits long-term variations in its timing and spectral parameters. In the period 2001–2003 the total flux stayed almost constant, whereas the blackbody temperature increased from ∼84 to over 94 eV, and also the pulse profile, the blackbody radius, and the equivalent width of the absorption feature changed. In the following years this trend appeared to reverse, with a decrease of the surface temperature. Two main explanations for this behavior were proposed: either free precession, which predicts a cyclic pattern (Haberl et al. 2006), or a glitch that occurred around MJD = 52866 ± 73 days (van Kerkwijk et al. 2007). According to the most recent analyses (Hohle et al. 2009, 2012b), the interpretation in terms of a single sudden event around the proposed glitch epoch seems favored.

In this Letter we reanalyze all the archival *XMM-Newton* observations of RX J0720.4–3125, performing a detailed phase-resolved spectral analysis. In Section 2 we report on the data analysis, and present the discovery of a second, new, phase-dependent absorption feature in the X-ray spectrum, the possible origin of which is discussed in Section 3.

2. *XMM-NEWTON* DATA ANALYSIS AND RESULTS

RX J0720.4–3125 was observed 20 times by the *XMM-Newton* satellite using the European Photon Imaging Camera (EPIC). We used here only data obtained with the EPIC-pn camera (Strüder et al. 2001) because less affected by pile-up (see Table 1). We processed the data using the Science Analysis Software (SAS, version 13.5.0), adopting the most recent calibration files available, and we removed any particle flare via good-time-intervals. All arrival times were referred to the Solar System barycenter (source coordinates R. A. = $07^{\rm h}20^{\rm m}24\overset{\rm s}{.}961$, decl. = $-31°25'50\overset{''}{.}21$, J2000.0;

Table 1
Summary of The *XMM-Newton*/EPIC-pn Observations of RX J0720.4–3125[a]

Obs. ID	Obs. Date YYYY MM DD	Read-out Mode/Filter	Live Time (ks)	Source Net Count Rate (counts s^{-1})	Pile-up Fraction Ratios $r = 0''$–$30''$
0124100101	2000 May 13	FF/thin	42.8	6.46(1)	0.963(3)
0132520301	2000 Nov 21	FF/medium	22.7	5.60(2)	0.964(4)
0156960201	2002 Nov 06	FF/thin	25.6	6.60(2)	0.969(3)
0156960401	2002 Nov 08	FF/thin	27.1	6.54(2)	0.966(3)
0158360201	2003 May 02	SW/thick	51.0	3.480(8)	1.011(3)
0161960201	2003 Oct 27	SW/thin	12.6	7.52(2)	1.013(5)
0164560501	2004 May 22	FF/thin	32.0	6.96(1)	0.971(3)
0300520201	2005 Apr 28	FF/thin	38.1	6.86(1)	0.968(3)
0300520301	2005 Sep 22	FF/thin	39.1	6.93(1)	0.969(3)
0311590101	2005 Nov 12	FF/thin	33.5	6.75(1)	0.970(3)
0400140301	2006 May 22	FF/thin	17.6	6.83(2)	0.970(4)
0400140401	2006 Nov 05	FF/thin	17.6	6.90(2)	0.966(4)
0502710201	2007 May 05	FF/thin	17.4	6.80(2)	0.968(4)
0502710301	2007 Nov 17	FF/thin	20.1	7.71(2)	0.971(4)
0554510101	2009 Mar 21	FF/thin	16.7	6.84(2)	0.967(4)
0601170301	2009 Sep 22	FF/thin	15.0	6.77(2)	0.968(4)
0650920101	2011 Apr 11	FF/thin	17.6	6.61(2)	0.973(4)
0670700201	2011 May 02	FF/thin	23.6	6.73(2)	0.965(3)
0670700301	2011 Oct 01	FF/thin	22.2	6.60(2)	0.972(3)
0690070201	2012 Sep 18	FF/thin	22.3	6.60(2)	0.970(3)

Note.
[a] FF: full frame (time resolution of 73 ms); SW: small window (time resolution of 6 ms). Live time refers to the duration of the observations after filtering for background flares (see the text). Count rates refer to the spectra extracted within a circular region with PATTERN = 0. Errors on the count rates are quoted at the 1σ confidence level. Pile-up fraction ratios were calculated for single events alone and in the 0.1–1.2 keV energy range using the `SAS epatplot` tool.

Kaplan et al. 2003), and a rotational phase was assigned to the source counts of all the observations using the timing solution of Hohle et al. (2012b). For the source distance we assumed $D = 286$ pc (Tetzlaff et al. 2011). All errors are reported at the 90% confidence level.

Spectral analysis was performed using the `XSPEC` analysis package (version 12.8.2; Arnaud 1996), using a minimum of 100 counts per bin for each spectrum, the χ^2 statistics and a maximum oversampling of the spectral energy resolution of a factor of 3. The fits were restricted to energies between 0.3 and 1.2 keV to exclude the broad absorption line at ~270 eV so as to reduce the number of degrees of freedom (dof). We extracted the source spectra from a circular region of radius 30″ centered on the source point-spread function and the background counts from a circle of the same size far from the source and on the same CCD. For small window and full frame observations the pile-up level, estimated by means of the SAS `epatplot` tool, was <1.5% and 4%, respectively (see Table 1). To mitigate the pile-up we restricted our spectral analysis to photons having FLAG = 0 and PATTERN = 0.

We started our analysis from the 2003 May 2 observation, this being the longest observation, and least affected by pile-up (the pn was operating in Small Window mode). The phase-averaged spectrum is well fitted by an absorbed[10] blackbody (reduced chi-square $\chi^2_\nu = 1.17$ for 130 dof) yielding the following parameters: column density $N_{\rm H} = 1.9(3) \times 10^{20}$ $\rm cm^{-2}$, blackbody temperature $kT_{\rm BB} = 82.1 \pm 0.6$ eV and blackbody radius $R_{\rm BB} = 6.3 \pm 0.6$ km.

[10] We took into account the effects of interstellar absorption along the line of sight through the `TBABS` model with the `vern` cross sections (Verner et al. 1996) and the `wilm` abundances (Wilms et al. 2000).

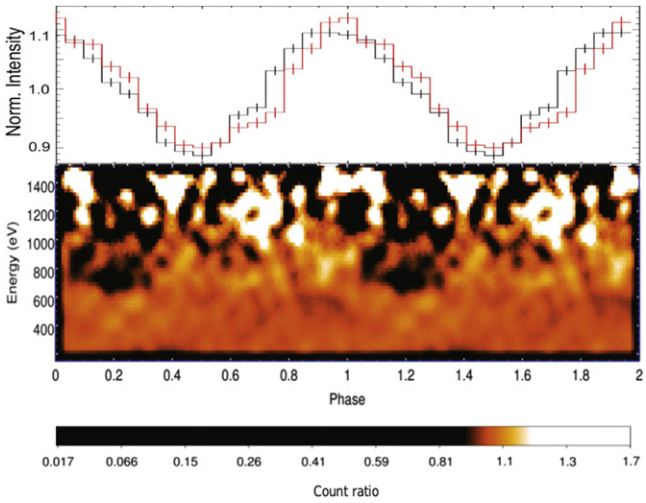

Figure 1. Top panel: pulse profile for the 2003 May 2 observation (red) and for all observations merged together (black). Bottom panel: normalized energy vs. phase image obtained by binning the EPIC source counts into 0.01 phase bins and 25 eV energy channels for the observation performed on 2003 May 2.

To study in detail the spectral variability with phase, we produced a phase-energy image by binning the EPIC-pn source counts into 100 rotational phase channels and 25 eV wide energy channels, and then normalizing to the phase-averaged energy spectrum. The image (Figure 1) shows a feature in the phase interval 0.1–0.3, which gives a strong hint for the presence of an absorption line at ~750 eV in the corresponding spectrum. Above ~1 keV the source counts become background dominated.

Table 2
Pulse Phase Spectroscopy For 2003 May 2 Observation

Parameter[a]	0.1–0.3	0.3–0.5	0.5–0.7	0.7–0.9	0.9–1.1
			BB		
kT_{BB} (eV)	81.1(6)	81.9(6)	82.2(6)	82.6(6)	82.5(9)
R_{BB} (km)	$6.4^{+0.6}_{-0.5}$	$6.0^{+0.6}_{-0.5}$	$6.1^{+0.6}_{-0.5}$	$6.4^{+0.6}_{-0.5}$	$6.4^{+0.7}_{-0.6}$
Flux[b]	0.86(1)	0.82(1)	0.86(1)	0.95(1)	0.95(1)
Unabs. Flux[b]	1.07	1.01	1.06	1.17	1.17
NHP[d]	7.2×10^{-2}	5.9×10^{-1}	6.9×10^{-1}	4.2×10^{-2}	2.7×10^{-1}
χ^2_ν	1.22	0.96	0.92	1.26	1.09
dof	92	90	92	97	75
			BB+GAUSS		
kT_{BB} (eV)	$83.0^{+1.5}_{-0.9}$	82.4(9)	$82.2^{+0.7}_{-0.6}$	82.7(8)	$82.4^{+1.0}_{-0.9}$
R_{BB} (km)	6.0(6)	$6.0^{+0.6}_{-0.5}$	$6.1^{+0.6}_{-0.5}$	$6.3^{+0.6}_{-0.5}$	6.4(6)
E_{line} [c] (eV)	745^{+17}_{-27}	745	745	745	745
σ [c](eV)	$41.7^{+51.3}_{-33.8}$	41.7	41.7	41.7	41.7
|Norm|	$9.2^{+3.5}_{-9.2} \times 10^{-5}$	$\leqslant 2.7 \times 10^{-5}$	$\leqslant 1.7 \times 10^{-5}$	$\leqslant 2.9 \times 10^{-5}$	$\leqslant 2.4 \times 10^{-5}$
Eq. Width (eV)	28^{+9}_{-11}	6^{+9}_{-5}	$\leqslant 8$	$\leqslant 11$	$\leqslant 13$
F-test (10^{-3})	3.5×10^{-7}	232	1000	750	>1000
NHP[d]	7.9×10^{-1}	6.0×10^{-1}	6.6×10^{-1}	3.6×10^{-2}	2.5×10^{-1}
χ^2_ν	0.88	0.95	0.93	1.27	1.11
dof	89	89	91	96	74

Notes.
[a] N_H was frozen at the value obtained for the phase averaged spectra: $N_H = 1.9 \times 10^{20}$ cm^{-2} .
[b] Fluxes are calculated in the 0.3–1.2 keV energy range and in units of (10^{-11} erg s^{-1} cm^{-2}).
[c] Line energy and width were frozen at the value obtained for the phase interval 0.1–0.3: $E_{line} = 745$ eV and $\sigma = 42$ eV.
[d] NHP is the Null Hypothesis Probability.

To better investigate the significance of the feature appearing in Figure 1, we performed a phase-resolved spectral analysis for the 2003 May 2 observation dividing the rotational cycle in five equal phase bins. For the spectrum relative to phase 0.1–0.3 the addition of a Gaussian line in absorption to the blackbody continuum leads to a significant improvement in the shape of residuals, while a simple blackbody model gives an acceptable fit for all the other phase bins. Both the `gabs` and `Gauss` models result in $\chi_\nu^2 = 0.88$ for 89 dof, corresponding to an F-test probability of 3.5×10^{-7}. We multiplied this value by 5, considering the five phase-intervals as trials. In this way we obtained a significance of $\sim 5\sigma$. The values for line energy and width, obtained from the two models, are compatible within the errors. The best-fit `tbabs*(bbodyrad+Gauss)` model gave the following parameters: $kT_{BB} = 83.0 \pm 0.1$ eV, $R_{BB} = 6.3 \pm 0.3$ km, line energy $E_{line} = 745^{+17}_{-27}$ eV, width $\sigma = 42^{+51}_{-33}$ eV and normalization of $-9.2^{+3.5}_{-9.2} \times 10^{-5}$ (the column density was frozen at the value obtained for the phase-averaged spectrum). The equivalent width of the feature is 28^{+9}_{-11} eV. Table 2 summarizes the results of the phase-resolved spectroscopy for the 2003 May 2nd observation using the `tbabs*(bbodyrad+Gauss)` model. Figure 2 shows the phase-resolved spectrum relative to phase 0.1–0.3 (black) in comparison with that at phase 0.5–0.7 (red): the absorption feature clearly shows up in the residuals.

The same phase-averaged and phase-resolved analysis was then repeated for all the remaining *XMM-Newton* observations in search for the presence of the 745 eV absorption line. Since

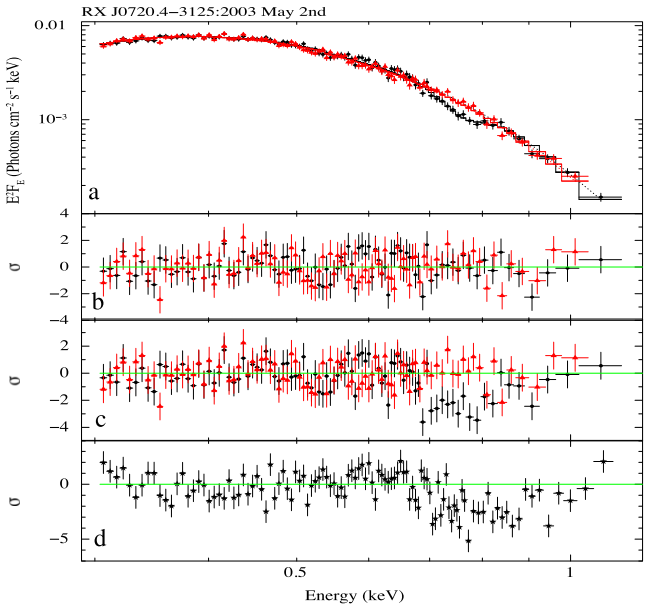

Figure 2. From top to bottom. Panel (a): spectrum of the 0.1–0.3 phase interval (black circles) fitted with an absorbed blackbody plus a Gaussian profile (`Gauss` model); the spectrum in the phase range 0.5–0.7 together with the best fitting model (`tbabs*bbodyrad`) is also shown (red triangles). Both spectra are from the 2003 May 2 observation. Panel (b): residuals with respect to these models. Panel (c): residuals of the previous spectra after setting the line normalization to zero. Panel (d): residuals of the spectrum relative to phase 0.1–0.3 after merging the phase-resolved spectra of all observations listed in Table 1.

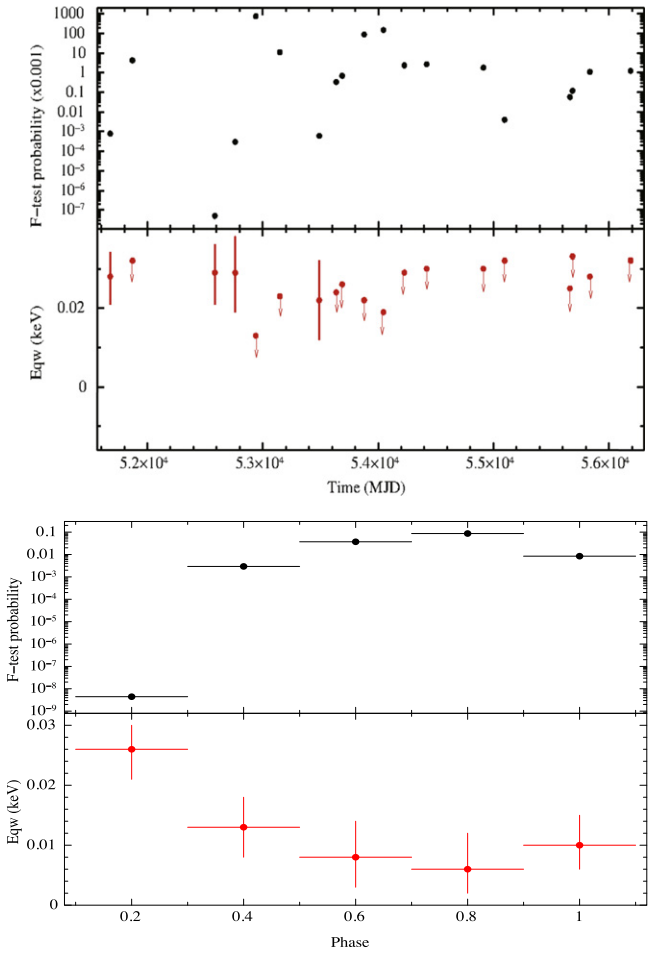

Figure 3. Top panel: evolution of the F-test probability and line equivalent width with time for the spectra in the 0.1–0.3 phase range for all *XMM-Newton* observations (the two observations performed during 2002 November were merged being only two days apart). Bottom panel: F-test probability and equivalent width as a function of the spin phase for the spectrum of all merged observations.

observations in Full Frame mode were affected by pile-up, their spectra were extracted from an annular region extending from 15″ to 30″ from the nominal source position, this time including also events with PATTERN ⩽ 4. The resulting values of the line equivalent width and the F-test probability as a function of time are shown in Figure 3 (top panel), and clearly indicate that the presence of the feature is unconstrained in most of the observations, possibly because of their lower statistics.

We then performed a simultaneous fit of the spectra in the 0.1–0.3 phase bin for all the observations in Full Frame mode with the Thin filter (18 spectra in total; see Table 1). We constrained $N_{\rm H}$ and the line energy to be the same (to minimize the free parameters), and the width of the feature was frozen at the value obtained for the 2003 May observation. The phase-dependent feature is detected at an energy of 785(13) eV for the `tbabs*(bbodyrad+Gauss)` model ($\chi^2_\nu = 0.96$ for 556 dof); normalizations and equivalent widths are consistent within the errors in all the spectra. The `tbabs*bbodyrad` model gives $\chi^2_\nu = 1.03$ for 575 dof. The F-test probability for the inclusion of the Gaussian absorption line is 4.2×10^{-6}, which corresponds to a significance level of $\sim 4.5\sigma$ (taking into account the number of trials).

To further test the presence of this feature in data taken before and after 2003 May 2, we also combined all the spectra except that of 2003 May 2. We used the `SAS epicspec-combine` tool to merge the spectra and the response matrices. For the combined spectrum in the phase range 0.1–0.3, the best-fit with a blackbody model yields $\chi^2_\nu = 2.04$ for 123 dof; by including a Gaussian absorption line, χ^2_ν decreases to 1.48 for 121 dof. The parameters for the phase-dependent line are: $E_{\rm line} = 795\ ^{+15}_{-14}$ eV, normalization of $(-8.3\ ^{+1.7}_{-1.7}) \times 10^{-5}$ and equivalent width of 27^{+6}_{-5} eV for the `Gauss` model (the line width was fixed to the value obtained from the 2003 May 2 observation). The F-test probability between these two models is 1.3×10^{-9} and the significance is equal to 6σ (again considering 5 trials).

As a further check, we built a combined spectrum comprising all observations. This spectrum, created by merging all the spectra extracted from a 15″ to 30″ annular region with PATTERN ⩽ 4, has an exposure time of 406.8 ks and a much improved statistics. The 0.1–0.3 phase-resolved spectrum shows an absorption feature at energy 787^{+15}_{-14} eV with normalization of $-7.9^{+1.6}_{-1.7} \times 10^{-5}$ and equivalent width of 26^{+4}_{-5} eV for the `Gauss` model; also in this case we froze the line width at the value estimated for the longest observation. The F-test probability for the inclusion of the absorption feature is now 4.7×10^{-9} and, taking into consideration the number of trials, the significance level is again $\sim 6\sigma$. As shown in Figure 2, panel (d), the spectral feature is clearly detectable in the fit residuals of the merged observations, and the line significance increases with respect to the 2003 May observation alone.

In the spectra relative to the other phase intervals the line equivalent width is always <13 eV, and the F-test probability is never $<3 \times 10^{-3}$ (see Figure 3, lower panel). We stress that the response of the pn camera has slightly changed (see, e.g., Sartore et al. 2012) over the 12 years spanned by the observations, hence mixing spectra obtained with different settings over such a long period certainly introduce large systematic errors which are difficult to quantify. However, a spectral feature present only in a given phase interval cannot result from systematic effects, which are definitely independent on the rotational phase. While the line is mostly evident in the 2003 May 2 observation, which we used to derive the best estimate of the line parameters, the considerations presented above strongly suggest that the feature was present also in the other observations, with properties which appear relatively stable over the 12 year period covered by *XMM-Newton* data.

3. DISCUSSION

A careful re-analysis of all available *XMM-Newton* observations of the isolated neutron star RX J0720.4–3125 revealed the presence of a phase-dependent absorption feature at ∼750 eV, which is mostly evident during the decline of the pulse profile (phases 0.1–0.3). The feature was first significantly detected (at $\sim 5\sigma$ confidence level) in the 2003 May 2 *XMM-Newton* observation, which was the longest one and was less affected by pile-up. Phase-dependent spectral analysis of the remaining datasets, which cover the period 2000 May–2012 September, indicates that the feature is likely present at all epochs and its properties are consistent with being constant over the timespan covered by available observations (∼12 years). This suggests that the feature may be long-lasting and not associated with the timing anomalies (possibly due to a

glitch) that occurred in 2003 (van Kerkwijk et al. 2007; Hohle et al. 2012b).

Interestingly, an absorption feature with somewhat similar properties has been discovered in the spectrum of the "low-field" magnetar SGR 0418+5729 ($B_{\rm dip} \sim 6 \times 10^{12}$ G; Tiengo et al. 2013). In both cases the feature is present only in a quite narrow phase interval ($\sim$1/5 of the phase cycle), but in SGR 0418+5729 the line energy is higher ($\gtrsim$2 keV) and strongly variable in phase (by a factor $\sim$5 in one-tenth of the phase cycle). No clear variation of the line energy with phase is seen in RX J0720.4–3125, although this might simply reflect the fact that the source counts become background dominated at energies just above that of the feature. Tiengo et al. (2013) interpreted the feature in SGR 0418+5729 as due to proton cyclotron resonant scattering in a baryon-loaded magnetic loop close to the star surface. The B-field variation along the loop explains the strong dependence of the line energy with phase, since photons emitted from the surface intersect the loop at different positions.

The similarities between the two features are suggestive that the same mechanism may be at work in RX J0720.4–3125. If the feature is a (broadened) proton cyclotron line, its energy is $E_{\rm line} = 0.63 (B_{\rm loop}/10^{14}\ {\rm G})/(1+z)$ keV, where $1/(1+z) \sim 0.7$ is the gravitational redshift at the star surface. The implied magnetic field in the loop is $B_{\rm loop} \sim 1.8 \times 10^{14}$ G, a factor of $\sim$7 larger than the the equatorial value of the dipole magnetic field at the surface, $B_{\rm dip} \sim 2.5 \times 10^{13}$ G. A preliminary calculation using the same geometrical model as in Tiengo et al. (2013) shows that the energy of the line and its appearance only for $\sim$20% of the star period can indeed be reproduced. It should be noted, however, that the exact geometry of the magnetic structure is likely different in the two sources. In the case of SGR 0418+5729, in fact, X-ray photons come from a quite small, hot spot with size $\sim$1 km, while the emitting region of RX J0720.4–3125, albeit not uniform, is larger ($R_{\rm BB} \sim 6$ km).

A further possibility is that the line results from atomic absorption in the neutron star (magnetized) atmosphere. The strong dependence of the feature on the star rotational phase may be due to local inhomogeneities in the star surface magnetic field (as in the cyclotron scenario above) and/or to a clumpy structure of the atmosphere itself. The possibility that primary photons come from a small hot spot appears, on the other hand, unlikely, given the relatively large radiation radius and the broad shape of the pulse profile. If the feature arises from bound-bound (or bound-free) transitions, the atmosphere composition is most probably He or mid-Z elements (see, e.g., Pavlov & Bezchastnov 2005; Mori & HO 2007). The ionization energy for H is, in fact, below $\sim$0.7 keV for fields $\lesssim 10^{14}$ G (above this value the feature may be washed out by vacuum resonance mode conversion; e.g., van Kerkwijk & Kaplan 2007 and references therein).

The presence of proton cyclotron lines produced by resonant scattering/absorption in confined, high-B structures close to the star surface, where the magnetic field is a factor $\gtrsim$10 higher than the dipole, would be supportive of a picture in which the magnetic field of (highly magnetized) neutron stars is complex, with substantial deviations from a pure dipole on the small scales. In recent years, a better (although far from conclusive) understanding of how stellar magnetic fields are generated and amplified indicates that strong, non-dipolar field components are ubiquitous, from massive stars (Braithwaite & Spruit 2006) to proto-neutron stars (Obergaulinger et al. 2014). It is now well established that internal toroidal field components, multipolar surface structures, as well as very localized B-field bundles must be present in many neutron stars, especially in highly magnetized ones. The recent discovery of sources showing strong magnetic-powered flares and outbursts, but with low dipolar magnetic fields, $\lesssim 10^{13}$ G, further strengthens this idea (Rea et al. 2010, 2012, 2014; Turolla & Esposito 2013).

Finally, we stress that the absorption feature reported here for the first time is unlikely related to the broad absorption feature at 270 eV (Haberl et al. 2004, 2006). Even if the two may have the same physical origin, i.e., a proton cyclotron resonance, the latter implies a lower magnetic field, $\sim 5 \times 10^{13}$ G, comparable to the spin-down estimate, $B_{\rm dip} \sim 2.4 \times 10^{13}$ G, indicating that in this hypothesis it is related to the large-scale field. Actually broad absorption features have been detected in all the XDINSs, with the exception of RX J1856.5–3754 (e.g., Turolla 2009), but the strong phase variability we observe for the 0.75 keV line of RX J0720.4–3125 sets it apart.

This is the first time evidence of a complex magnetic field structure is observed in an XDINS, although this result is not unexpected, if, as suggested by many investigations, XDINSs are aged magnetars (Viganò et al. 2013; see also Turolla 2009).

A.B., N.R., and F.C.Z are supported by an NWO Vidi Grant (PI: Rea) and by the European COST Action MP1304 (NewCOMPSTAR). N.R. acknowledges support by grants AYA2012-39303 and SGR2014-1073. The work of R.T. and A.T. is partially supported by an INAF PRIN grant.

REFERENCES

Arnaud, K. A. 1996, in ASP Conf. Ser. 101, Astronomical Data Analysis Software and Systems V, ed. G. H. Jacoby & J. Barnes (San Francisco, CA: ASP), 17
Braithwaite, J., & Spruit, H. 2006, A&A, 450, 1097
Haberl, F., Motch, C., Buckley, D. A. H., Zickgraf, F.-J., & Pietsch, W. 1997, A&A, 326, 662
Haberl, F., Zavlin, V. E., Trümper, J., & Burwitz, V. 2004, A&A, 419, 1077
Haberl, F., et al. 2006, A&A, 451, L17
Hohle, M. M., Haberl, F., Vink, J., de Vries, C. P., & Neuhäuser, R. 2012a, MNRAS, 419, 1525
Hohle, M. M., Haberl, F., Vink, J., et al. 2009, A&A, 498, 811
Hohle, M. M., Haberl, F., Vink, J., et al. 2012b, MNRAS, 423, 1194
Kaplan, D. L., van Kerkwijk, M. H., Marshall, H. L., et al. 2003, ApJ, 590, 1008
Mori, K., & HO, W. C. G. 2007, MNRAS, 377, 905
Obergaulinger, M., Janka, H.-T., & Aloy, M. A. 2014, MNRAS, 445, 3169
Pavlov, G. G., & Bezchastnov, V. G. 2005, ApJL, 635, L61
Rea, N., Esposito, P., Turolla, R., et al. 2010, Sci, 330, 944
Rea, N., Israel, G. L., Esposito, P., et al. 2012, ApJ, 754, 27
Rea, N., Viganò, D., Israel, G. L., Pons, J. A., & Torres, D. F. 2014, ApJL, 781, L17
Sartore, N., Tiengo, A., Mereghetti, S., et al. 2012, A&A, 541, A66
Strüder, L., Briel, U., Dennerl, K., et al. 2001, A&A, 365, 18
Tetzlaff, N., Eisenbeis, T., Neuhäuser, R., & Hohle, M. M. 2011, MNRAS, 417, 617
Tiengo, A., Esposito, P., Mereghetti, S., et al. 2013, Natur, 500, 312
Turolla, R. 2009, Astrophysics and Space Science Library, 357, 141
Turolla, R., & Esposito, P. 2013, IJMPD, 22, 30024
van Kerkwijk, M. H., & Kaplan, D. L. 2007, Ap&SS, 308, 191
van Kerkwijk, M. H., Kaplan, D. L., Pavlov, G. G., & Mori, K. 2007, ApJL, 659, L149
Verner, D. A., Ferland, G. J., Korista, K. T., & Yakovlev, D. G. 1996, ApJ, 465, 487
Viganò, D., Perna, R., Rea, N., & Pons, J. A. 2014, MNRAS, 443, 31
Viganò, D., Rea, N., Pons, J. A., et al. 2013, MNRAS, 434, 123
Wilms, J., Allen, A., & McCray, R. 2000, ApJ, 542, 914